Nanoscale assembly of amine-functionalized colloidal iron oxide

K.C. Barick [a], M. Aslam [b,f], Pottumarthi V. Prasad [c], Vinayak P. Dravid [d,e,*], Dhirendra Bahadur [a,f,**]

[a] Department of Metallurgical Engineering and Materials Science, Indian Institute of Technology Bombay, Mumbai 400076, India
[b] Department of Physics, Indian Institute of Technology Bombay, Mumbai 400076, India
[c] Department of Radiology, Evanston Northwestern Healthcare, Evanston, IL 60201, USA
[d] Department of Materials Science and Engineering, Northwestern University, Evanston, IL 60208, USA
[e] International Institute for Nanotechnology, Northwestern University, Evanston, IL 60208, USA
[f] Centre for Research in Nanotechnology and Science, Indian Institute of Technology Bombay, Mumbai 400076, India

ARTICLE INFO

ABSTRACT

We demonstrate a single-step facile approach for highly water-stable assembly of amine-functionalized Fe_3O_4 nanoparticles using thermal decomposition of Fe-chloride precursors in ethylene glycol medium in the presence of ethylenediamine. The average size of nanoassemblies is 40 ± 1 nm, wherein the individual nanoparticles are about 6 nm. Amine-functionalized properties are evident from Fourier transform infrared spectrometer (FTIR), thermal and elemental analyses. The saturation magnetization and spin-echo r_2 of the nanoassemblies were measured to be 64.3 emu/g and 314.6 $mM^{-1} s^{-1}$, respectively. The higher value of relaxivity ratio ($r_2/r_1 = 143$) indicates that nanoassemblies are a promising high-efficiency T2 contrast agent platform.

© 2009 Elsevier B.V. All rights reserved.

1. Introduction

Magnetic resonance imaging (MRI) is a powerful clinical tool for the non-invasive diagnosis and post-therapy assessment of variety of diseases. The MRI technique relies upon the relaxation of water protons that depends on the magnetic field, pulse sequence, heterogeneous distribution and surrounding environment of water in the organism [1,2]. The interpretation of the resulting MR image helps demarcate and identify most of the tissues. The contrast can be improved by using positive or negative contrast enhancers [3]; negative contrast agents induce a large shortening of the transverse relaxation time (T2) leading to a darkening of MR images, wherein the close contact of water molecules with positive contrast agent is reflected by a brightness that echoes the shortening of longitudinal relaxation time (T1).

Superparamagnetic iron oxide nanoparticles are the most promising T2 contrast agents for non-invasive *in vivo* monitoring of molecular and cellular events [4–6]. Most of the work in this area has been focused on multi-step surface functionalization of superparamagnetic iron oxide nanoparticles for MRI applications [5–8]. Recently, monodispersed magnetic nanoparticles, nanoassemblies (MNNA) made up of numerous superparamagnetic nanoparticles are attracting considerable interest because of their potential applications in MRI; iron oxide core of individual superparamagnetic nanoparticles in the nanoassembly becomes more efficient at dephasing the spins of surrounding water protons and hence enhances T2 relaxation time [9–11]. Of late, advances in chemical synthesis have enabled the preparation of high-quality functionalized nanoassemblies of tunable (size and shape) nanoparticles. This can lead to artificially enhanced relaxation properties generated by the accumulative interparticles interaction. Thus, self-aggregation or self-assembly through spatial arrangement of nanoparticles as building blocks is the fundamental mechanism by which different nanoparticle assembly motifs or even closed packed ordered structures are formed in materials. The forces that controlled the assembly are determined by competing noncovalent intramolecular or intraparticulate interactions such as electrostatic interaction [12], hydrogen bonding [13], van der Waals [14] and dipole–dipole interactions [15]. Thus, well-defined ordered structures obtained through the assembly of nanocrystalline building blocks provide new opportunities for optimizing, tuning and/or enhancing the properties and performance of the materials.

Here, we demonstrate an environmentally and economically preferable one-step green chemistry approach for synthesizing highly water-stable Fe_3O_4 nano-colloidal assemblies with enhanced T2 contrast properties as compared to commercially available contrast agent. Specifically, superparamagnetic amine-functionalized Fe_3O_4 MNNA were produced by thermal decomposition of the Fe-chloride precursors in biocompatible

ethylene glycol medium in the presence of ethylenediamine (EDA) molecules.

2. Materials and methods

All chemicals are of analytical grade and used as received. In a typical synthesis of amine-functionalized Fe_3O_4 nanoassemblies, 1 g of Fe-chloride precursors ($Fe^{2+}/Fe^{3+} = 1:2$), 2 g of sodium acetate and 7 ml ethylenediamine were added to ethylene glycol (30 ml), and stirred vigorously by a magnetic stirrer at 70 °C to obtain a clear homogeneous golden yellow coloured mixture. This reaction mixture was transferred into a round bottom flask and temperature was slowly increased to 197 °C under reflux, and reacted for another 6 h. The black-coloured precipitates were obtained by cooling the reaction mixture to room temperature and then thoroughly rinsed with water to remove the solvent and by-products. During each rinsing step, samples were separated from the supernatant using a permanent magnet.

X-ray diffraction (XRD) pattern was recorded on a Philips powder diffractometer PW3040/60 with Cu Kα radiation. The electron micrographs were taken by Hitachi HF 2000 transmission electron microscope (TEM) for particle size determination. The infrared spectra were recorded in the range 2000–400 cm^{-1} on a Fourier transform infrared spectrometer (FTIR, Magna 550 and Nicolet Instruments Corporation, USA). The thermogravimetric analysis (TGA) was performed by TA Instruments SDT Q600 analyzer. The elemental analysis was carried out by FLASH EA 1112 series CHNS (O) analyzer (Thermo Finnigan, Italy). The concentration of metal ions in the samples was obtained by ICP–AES (8440 Plasmalab; Labtam, Australia). The field-dependence magnetization (M vs. H), and temperature-dependence magnetization under zero-field cooled (ZFC) and field-cooled (FC) conditions in an applied field of 500 Oe were measured by Quantum Design PPMS. The Curie temperature (T_C) was determined in an applied field of 100 Oe using vibrating sample magnetometer (VSM, Model 7410; Lake Shore).

The T1 and T2 relaxation times (s) of the samples were measured for different concentrations of Fe_3O_4 nanoassemblies using a 3 T clinical MRI scanner (General Electric Healthcare, USA). The different concentrations of amine-functionalized Fe_3O_4 samples were prepared by diluting them with milli-Q water (resistance 18.2 MΩ). T1-weighted images were obtained with a multiple inversion recovery SE sequence (TR 2200 ms; TI 2100, 800, 400, 200 and 50 ms; matrix 512×512) and T2-weighted images were obtained with an FSE sequence. The r_1 and r_2 relaxivities (mM^{-1} s^{-1}) were calculated from the slope of the linear plots of 1/T1 and 1/T2 vs. Fe ion concentrations.

3. Results and discussion

The XRD pattern of amine-functionalized Fe_3O_4 MNNA samples (Fig. 1a) reveal single-phase Fe_3O_4 inverse spinel structure. The presence of sharp and intense peaks confirmed the formation of highly crystalline nanoparticles. Fig. 1b shows the TEM image of amine-functionalized Fe_3O_4 MNNA (inset: magnified TEM image of a single Fe_3O_4 MNNA). The electron micrographs show that spherical nanoassemblies are well defined, discrete and porous in nature. Each 'nanosized sphere' of an average size 40 ± 1 nm is made up of three-dimensional (3-D) spatially connected nanoparticles of average diameter of about 6 nm. These fine nanoparticles are presumably assembled spontaneously into porous spherical superstructure to minimize their surface energy. The formation of such spherical nanoassemblies may be dependent on
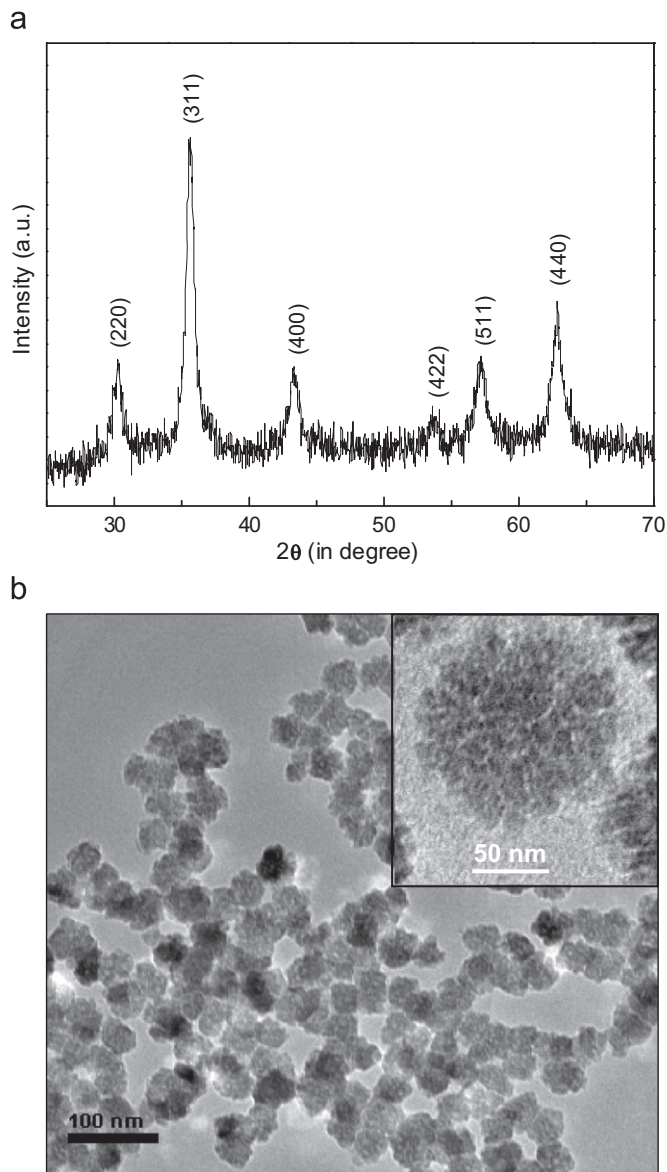

Fig. 1. (a) XRD pattern of amine-functionalized Fe_3O_4 MNNA samples (position and relative intensities of all diffraction peaks well matched with those from the Joint Committee on Powder Diffraction Standard (JCPDS) card 75-1609 of magnetite) and (b) TEM micrographs of amine-functionalized Fe_3O_4 MNNA samples (inset: magnified TEM image of a single Fe_3O_4 MNNA).

the collective behavior of nanoparticles and the intermolecular forces existing between them.

Fig. 2 shows the FTIR spectra of (a) ethylenediamine and (b) amine-functionalized Fe_3O_4 MNNA samples. The IR bands observed at around 588 cm^{-1} can be ascribed to the Fe–O vibrational mode of Fe_3O_4. The vibrational modes attributed to the free amine group such as NH_2 scissoring at 1595 cm^{-1}, C–N stretching at 1320 cm^{-1} and NH wagging at 932 cm^{-1} are clearly observed in the FTIR spectrum of amine-functionalized Fe_3O_4 nanoassemblies with a slight shift in their band positions.

Fig. 3 shows the TGA plot of amine-functionalized Fe_3O_4 MNNA samples. A weight loss of about 2.9% below 230 °C can be ascribed to the removal of diamine-modified glycol molecules attached to the surface of Fe_3O_4 MNNA and entrapped solvent from the porous network of nanoassemblies. The weight loss of about 2.3% between 230 and 310 °C may be associated with the transformation of Fe_3O_4 to γ-Fe_2O_3 phase upon thermal treatment [16].
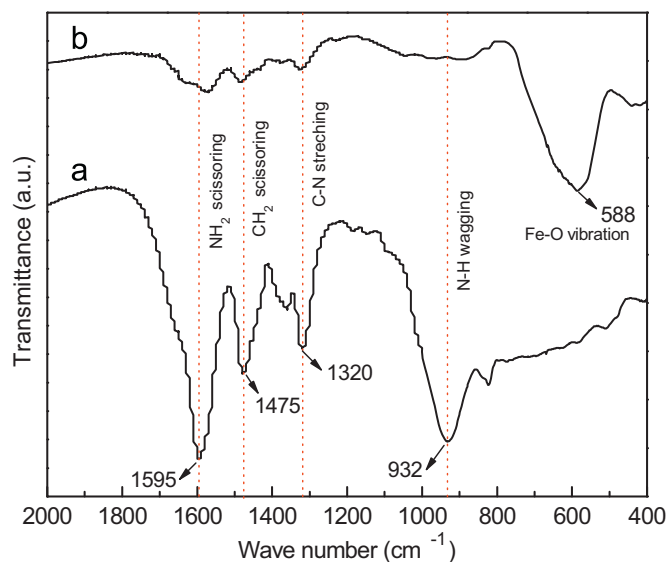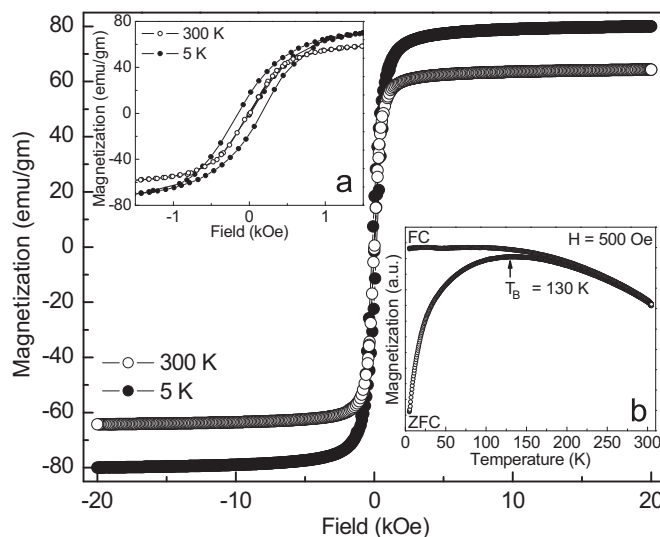
Fig. 2. FTIR spectra of (a) ethylenediamine and (b) amine-functionalized Fe_3O_4 MNNA samples.
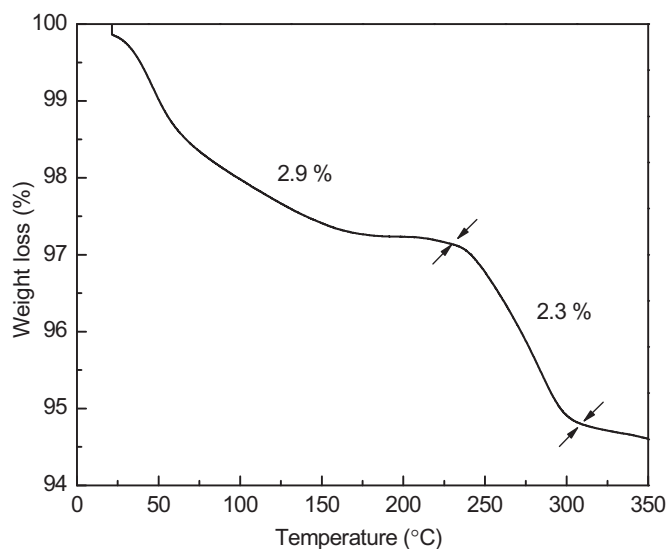
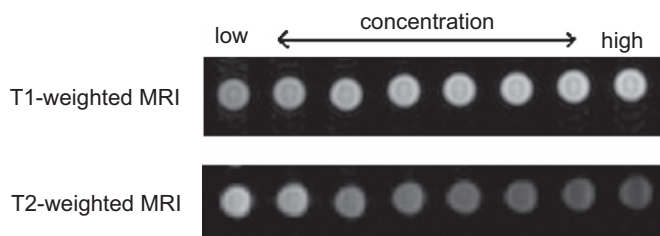**Fig. 3.** TGA plot of amine-functionalized Fe_3O_4 MNNA samples showing weight loss at different temperatures.

Fig. 4. M vs. H plot of amine-functionalized Fe_3O_4 MNNA. Inset: (a) its expanded M vs. H plot at the low-field region showing coercivity and (b) its ZFC–FC plot showing $T_B = 130$ K.

Fig. 5. T1-weighted and T2-weighted phantom images of amine-functionalized Fe_3O_4 MNNA with different Fe ion concentrations (from left: 0.006, 0.012, 0.025, 0.032, 0.039, 0.052, 0.065 and 0.097 mM).

Further, CHN elemental analysis of Fe_3O_4 MNNA clearly indicates the presence of organic components (3.011% C, 0.656% H and 0.63% N) on the samples. Thus, the FTIR, CHN and TGA results confirmed that Fe_3O_4 nanoparticles (MNNA) have been functionalized with amine groups during the synthesis. These amine-functionalized magnetic nanoassemblies were found to be highly stable in water. The 'colloidal' stability may be due to the formation of hydrogen bonds between the amine groups of functionalized magnetic nanoparticles and water.

Fig. 4 shows the M vs. H plot of amine-functionalized Fe_3O_4 MNNA at 5 and 300 K. At 300 K, samples exhibit superparamagnetic behavior without magnetic hysteresis and remanence whereas ferrimagnetic behavior with a coercivity of about 100 Oe is observed at 5 K (inset 'a' of Fig. 4). This transition from superparamagnetic behavior at high temperature to ferro or ferrimagnetic behavior below the so-called blocking temperature is typically observed in magnetic nanoparticles. The saturation magnetizations of amine-functionalized Fe_3O_4 samples were found to be 64.3 and 80.0 emu/g at 300 and 5 K, respectively. The ZFC–FC plot (inset 'b' of Fig. 4) shows that the blocking temperature (T_B) of the MNNA is 130 K, as one would expect for superparamagnetic nanoparticles. Further, the Curie temperature (T_C) of MNNA was found to be 853 K, which is in agreement with that reported for Fe_3O_4 whereas the T_C of γ-Fe_2O_3 is around 918 K [17–19]. These results suggest that the phase formed is Fe_3O_4 rather than γ-Fe_2O_3.

T1- and T2-weighted phantom images of amine-functionalized Fe_3O_4 MNNA with different Fe ion concentrations are shown in Fig. 5. It has been observed that T1 relaxation time decreases with increasing the Fe concentration from 0.006 to 0.097 mM, while T2 relaxation time reduces accordingly. The r_1 and r_2 relaxivities of amine-functionalized Fe_3O_4 nanoassemblies in water were found to be 2.2 and 314.6 mM^{-1} s^{-1}, respectively, and the relaxivity ratio, r_2/r_1 is 143 which is much higher than that of commercial contrast agents such as Resovist (SH U 555 A), Feridex (AMI-25) and Supravist (SH U 555 C) measured at 3 T [20] shown in Table 1. The higher the relaxivity ratio, the higher is the T2 effect and the signal decreases on T2-weighted images. Thus, the high value of relaxivity ratio of Fe_3O_4 MNNA indicates that these nanoassemblies are promising candidate for high-efficiency T2 contrast agents. Such a significant improvement in the T2 MR signal arises from the synergistic magnetism of multiple Fe_3O_4 nanoparticles of the assemblies. Further, the nanoassemblies formed by clustering of nanoparticles decrease the surface of iron oxide in contact with the solvent and hence decrease in the T1 relaxivity. The enhancement of T2 relaxivity reflects the ability of magnetic nanoassemblies to distort the local magnetic field effectively.

Table 1

The r_1 and r_2 relaxivities and relaxivity ratio (r_2/r_1) of Fe_3O_4 MNNA and commercial contrast agents: Resovist (SH U 555 A), Feridex (AMI-25) and Supravist (SH U 555 C) measured at 3 T [20].

Materials	Surface functionality	r_1 (mM^{-1} s^{-1})	r_2 (mM^{-1} s^{-1})	r_2/r_1
Fe_3O_4 MNNA	Amine-functionalized Fe_3O_4 superparamagnetic nanoassemblies	2.2	314.6	143
Resovist (SH U 555 A)	Carboxydextran-coated superparamagnetic iron oxide	4.6	143	31.0
Feridex (AMI-25)	Dextran-coated superparamagnetic iron oxide	4.1	93	22.6
Supravist (SH U 555 C)	Carboxydextran-coated superparamagnetic iron oxide	7.3	57	7.8

4. Conclusions

A new class of water-stable amine-functionalized Fe_3O_4 nanoassemblies has been synthesized by a simple and green approach; high-temperature decomposition of Fe-chloride precursors carried out in a biocompatible ethylene glycol medium in the presence of ethylenediamine molecules. The size of nanoassemblies is about 40 ± 1 nm while that of the individual nanoparticles is about 6 nm. The high value of saturation magnetization and relaxivity ratio indicates that these nanoassemblies are very promising high-efficiency T2 contrast agents. Further, these amine groups on Fe_3O_4 MNNA surface can provide accessible surface for routine conjugation of biomolecules through the well-developed bioconjugation chemistry for a number of biomedical applications, such as magnetic biolabeling, efficient bioseparation and contrast enhancement for magnetic resonance imaging.

References

[1] M. Bottrill, L. Kwok, N.J. Long, Chem. Soc. Rev. 35 (2006) 557.
[2] Pottumarthi V. Prasad, Am. J. Physiol. Renal Physiol. 290 (2006) F958.
[3] S. Aime, M. Botta, E. Terreno, Adv. Inorg. Chem. 57 (2005) 173.
[4] J.H. Lee, Y.M. Huh, Y.W. Jun, et al., Nat. Med. 13 (2007) 95.
[5] M. Aslam, E.A. Schultz, T. Sun, et al., Cryst. Growth Des. 7 (2007) 471.
[6] D.E. Sosnovik, M. Nahrendorf, R. Weissleder, Basic Res. Cardiol. 103 (2008) 122.
[7] Y.M. Huh, Y.W. Jun, H.T. Song, et al., J. Am. Chem. Soc. 127 (2005) 12387.
[8] N. Nitin, L.E.W. LaConte, O. Zurkiya, et al., J. Bio. Inorg. Chem. 9 (2004) 706.
[9] J. -F. Berret, N. Schonbeck, F. Gazeau, et al., J. Am. Chem. Soc. 128 (2006) 1755.
[10] J. Lee, Y. Lee, J.K. Youn, et al., Small 4 (2008) 143.
[11] Y.W. Jun, J.W. Seo, J. Cheon, Acc. Chem. Res. 41 (2008) 179.
[12] F. Caruso, R. Caruso, H. Möhwald, Science 282 (1998) 1111.
[13] A.K. Boal, F. Ilhan, J.E. DeRouchey, et al., Nature 404 (2000) 746.
[14] S.M. Scholz, R. Vacassy, L. Lemaire, et al., Appl. Organomet. Chem. 12 (1998) 327.
[15] A. Sukhanova, A.V. Baranov, D. Klinov, et al., Nanotechnology 17 (2006) 4223.
[16] R.M. Cornell, U. Schwertmann, The Iron Oxides, VCH, New York, 1996, p. 135.
[17] K.C. Barick, D. Bahadur, Bull. Mater. Sci. 29 (2006) 595.
[18] H. Liu, E.Y. Jiang, R.K. Zheng, et al., J. Phys.: Condens. Matter. 15 (2003) 8003.
[19] T. Ebisu, T. Watanabe, Phys. Rev. D 36 (1987) 3359.
[20] M. Rohrer, H. Bauer, J. Mintorovitch, et al., Invest. Radiol. 40 (2005) 715.